Antonie van Leeuwenhoek (2013) 104:913–924
DOI 10.1007/s10482-013-0010-6

ORIGINAL PAPER

Metabolic and transcriptional response of *Escherichia coli* with a NADP$^+$-dependent glyceraldehyde 3-phosphate dehydrogenase from *Streptococcus mutans*

Sara Centeno-Leija · José Utrilla · Noemí Flores · Alberto Rodriguez · Guillermo Gosset · Alfredo Martinez

Received: 16 July 2013 / Accepted: 17 August 2013 / Published online: 29 August 2013
© Springer Science+Business Media Dordrecht 2013

Abstract The NAD$^+$-dependent glyceraldehyde-3-phosphate-dehydrogenase (NAD$^+$-GAPDH) is a key enzyme to sustain the glycolytic function in *Escherichia coli* and to generate NADH. In the absence of NAD$^+$-GAPDH activity, the glycolytic function can be restored through NADP$^+$-dependent GAPDH heterologous expression. Here, some metabolic and transcriptional effects are described when the NAD$^+$-GAPDH gene from *E. coli* (*gapA*) is replaced with the NADP$^+$-GAPDH gene from *Streptococcus mutans* (*gapN*). Expression of *gapN* was controlled by the native *gapA* promoter (*E. coli*Δ*gapA*::*gapN*) or by the constitutive *trc* promoter in a multicopy plasmid (*E. coli*Δ*gapA*::*gapN*/pTrcgapN). The specific NADP$^+$-GAPDH activity was 4.7 times higher in *E. coli*Δ*gapA*::*gapN*/pTrcgapN than *E. coli*Δ*gapA*::*gapN*. Growth, glucose consumption and acetic acid production rates increased in agreement with the NADP$^+$-GAPDH activity level. Analysis of *E. coli*Δ*gapA*::*gapN*/pTrcgapN showed that although *gapN* expression complemented NAD$^+$-GAPDH activity, the resulting low NADH levels decreased the expression of the respiratory chain and oxidative phosphorylation genes (*ndh*, *cydA*, *cyoB* and *atpA*). In comparison with the wild type strain, *E. coli*Δ*gapA*::*gapN*/pTrcgapN decreased the percentage of mole of oxygen consumed per mole of glucose metabolized by 40 % with a concomitant reduction of 54 % in the ATP/ADP ratio. The cellular response to avoid NADPH excess led to the overexpression of the transhydrogenase coded by *udhA* and the down-regulation of the pentose-phosphate and Krebs cycle genes, which reduced the CO_2 production and increased the acetic acid synthesis. The *E. coli* strains obtained in this work can be useful for future metabolic engineering efforts aiming for the production of metabolites which biosynthesis depends on NADPH.

Keywords *Escherichia coli* · NAD(P)$^+$-dependent glyceraldehyde-3-phosphate-dehydrogenase · Respiration · ATP · NAD(P)(H)

S. Centeno-Leija · J. Utrilla · N. Flores · A. Rodriguez · G. Gosset · A. Martinez (✉)
Departamento de Ingeniería Celular y Biocatálisis, Instituto de Biotecnología, Universidad Nacional Autónoma de México, Apartado postal 510-3, 62210 Cuernavaca, MOR, Mexico
e-mail: alfredo@ibt.unam.mx

Introduction

During glucose consumption, NADH generation in *Escherichia coli* is conducted through the Embden-Meyerhof-Parnas pathway (EMP) by the NAD$^+$-dependent glyceraldehyde-3-phosphate-dehydrogenase (NAD$^+$-GAPDH) (E.C. 1.2.1.12) enzyme encoded by *gapA* (D′Alessio and Josse 1971; Charpentier and Branlant 1994). NAD$^+$-GAPDH activity is essential to growth and is known to have higher relative activity compared to other enzymes in the EMP pathway (Charpentier and Branlant 1994; Thouvenot et al.

2004). In fact, it has been reported that controlling the expression of *gapA* allows modulation of the NAD^+-GAPDH activity and therefore the carbon flux trough the EMP pathway (Cho et al. 2012). Under aerobic conditions the main role of NADH is to generate ATP by oxidative phosphorylation in the respiratory chain and it is also required for more than 300 reduction reactions (Foster et al. 1990). On the other hand, in anaerobiosis NADH leads to fermentation reactions to maintain the redox balance in absence of oxygen as a final electron acceptor (Moat et al. 2002). Therefore, negative growth effects are observed when the NADH levels are altered, mainly by redox stress (Kim et al. 2009, 2011). Furthermore, *E. coli* mutants without NAD^+-GAPDH activity are unable to grow in the presence of hexoses, presumably due to the toxic accumulation of intermediates (Hillman and Fraenkel 1975; Irani and Maitra 1977).

Several genera of microorganisms, such as *Bacillus*, *Streptococcus* and *Clostridium*, have a $NADP^+$-GAPDH enzyme (E.C. 1.2.1.9) in addition to a NAD^+-GAPDH enzyme, allowing the production of NADH and NADPH through the EMP (Iddar et al. 2005). Since some species of *Streptococcus* lack the oxidative branch of the pentose phosphate pathway (PPP), the $NADP^+$-GAPDH activity is used as an alternative mechanism to generate NADPH (Brown and Wittenberger 1971). Unlike NAD^+-GAPDH, $NADP^+$-GAPDH does not require inorganic phosphate and this reaction is cooperative and irreversible. Specifically, the $NADP^+$-GAPDH enzyme from *Streptococcus mutans* coded by the *gapN* gene (Boyd et al. 1995) has a substrate affinity 10 times higher towards glyceraldehyde-3-P than the NAD^+-GAPDH enzyme GapA from *E. coli*, nevertheless $NADP^+$-GAPDH displays a strong inhibition by substrate and NADPH (Crow and Wittenbergerg 1979; Habenicht 1997; Marchal and Branlant 2002).

It has been demonstrated that some genes encoding $NADP^+$-GAPDH enzymes can complement an *E. coli* mutant deficient in native NAD^+-GAPDH (Fillinger et al. 2000; Iddar et al. 2002, 2003). These mutants are able to grow under aerobic conditions despite the decrease in the NADH levels necessary for energy generation, but not in anaerobic conditions, possibly due to the inability of the cell to sustain an efficient redox balance (Valverde et al. 1999; Martínez et al. 2008). Martinez and co-workers reported that the replacement of NAD^+-GAPDH from *E. coli* with a $NADP^+$-GAPDH enzyme from *Clostridium acetobutyricum* (GapC) increased the NADPH yield on glucose 1.7 times (Martínez et al. 2008) and a metabolic flux analysis revealed that the oxidative PPP branch and tricarboxylic acid cycle (TCA) fluxes were significantly reduced in the mutant Δ*gapA*::*gapC*, presumably to avoid high NADPH levels. Accordingly, heterologous lycopene production, a NADPH-dependent metabolite, increased 2.5 times in rich medium (Martínez et al. 2008). In fact, because *E. coli* has a limited capacity to generate NADPH through catabolic reactions (Csonka and Fraenkel 1977; Sauer et al. 2004; Fuhrer and Sauer 2009) the production of NADPH through the EMP could be exploited to produce NADPH-dependent metabolites of industrial interest, such as lycopene, caprolactone, L-lysine and polyhydroxybutyrate (Martínez et al. 2008; Takeno et al. 2010; Kim et al. 2011; Kocharin et al. 2013). However, the physiological effects resulting from the replacement of GAPDH activity and the concomitant production of NADPH through the EMP pathway has not been extensively studied in *E. coli*. In this work, a quantitative analysis was performed with data obtained from kinetic parameters, respiration rates, ATP/ADP and NAD(P)/NAD(P)H ratios and transcriptional data, providing further insights on the physiological response of *E. coli* to the replacement of NAD^+-GAPDH with a $NADP^+$-GAPDH from *S. mutans* when growing under aerobic conditions on glucose mineral media.

Materials and methods

Bacterial strains and plasmids

The wild-type *E. coli* MG1655 (GenBank NC 000913) was used as the parental strain and *S. mutans* (provided by the Culture Collection of the Faculty of Chemistry of the Universidad Nacional Autónoma de México) was used as a source of DNA for *gapN* amplification.

All plasmids and primers used in this work are listed in Table 1. Standard procedures were employed for plasmid preparations, restriction-enzyme digestions, transformations and gel electrophoresis (Sambrook and Rusell 2001). Each plasmid construction and mutants were verified by their restriction pattern in agarose gels and by sequencing. The chromosomal DNA was isolated with the Ultra Clean Microbial

Table 1 Plasmids and primers used in this work

Plasmid	Description	Source
pTrc99A	Designed for IPTG-inducible expression of proteins under the control of the hybrid trp/lac promoter. Amp^r	Amann et al. (1988)
pACYC184	Designed with p15A origin of replication to coexist in cells with plasmids of the ColE1 compatibility group (e.g., pBR322, pUC19). Tc^r and Cm^r	Chang and Cohen (1978)
pTgapN/cat-frt	pTrc99A derivative with the *gapN* gene fused with the *cat-frt* fragment	This study
pGapN	pTrc99A derivative containing the *gapN* gene	This study
pTrcgapN	pACYC184 derivative with trc promoter and *gapN* gene	This study
pKD46	Designed to inactivate chromosomal gene through phage λ Red recombinase	Datsenko and Wanner (2000)
pKD3	Designed to contain an FRT-flanked chloramphenicol resistance (cat) gene	Datsenko and Wanner (2000)
pCP20	Designed to remove FRT-flanked resistance markers	Cherepanov and Wackernagel (1995)

Primer	Sequence[a]
gapN1	5′ CATGCCATGGCAATGACAAAACAATATAAAAATTA 3′
gapN2	5′ CGGGGTACCCCGTTATTTGATATCAAATACGACGG 3′
Trc1	5′ GCCGACATCATAACGGTTCTGG 3′
cm1	5′ CGGGGTACCTGTAGGCTGGAGCTGCTTCG 3′
cm2	5′ TCCCCCCGGG CATATGAATATCCTCCTTA 3′
D1[b]	5′**GTAATTTTACAGGCAACCTTTTATTCACTAACAAATAGCTGGTGGAATAT**ATG ACAAAACAATATAAAAATTATG 3′
D2[b]	5′**AAAAAAGAGCGACCGAAGTCGCTCTTTTTAGATCACAGTG TCATCTCAAC**CATATGAATATCCTCCTTAGTTCCT 3′

[a] Restriction sites employed during plasmid construction are underlined

[b] Sequences that flank ~580 pb upstream and downstream of *gapA* gen are indicated in bold

DNA Isolation kit (MO BIO laboratories, Inc, Carlsbad, CA, USA). Gene amplifications were carried out by PCR on a C1000 Touch Thermal Cycler Manual (Bio-Rad Laboratories, Inc., Berkeley, CA, USA) using Expand High Fidelity polymerase (Roche Diagnostics GmbH, Mannheim, Germany). DNA fragments were isolated from agarose gels with the Roche Pure PCR Product Purification kit (Roche Diagnostics GmbH, Mannheim, Germany) according to the manufacturer's instructions.

The *gapA* gene (GenBank gene ID947679) from *E. coli* MG1655 was replaced by the gene *gapN* from *S. mutans* (GenBank Accession No. L38521). The MG1655*ΔgapA::gapN* mutant strain was made using a variation of the method reported by Datsenko and Wanner (2000) through the fusion of the *gapN* gene with a chloramphenicol resistance cassette. Using *S. mutans* chromosomal DNA as a template, the *gapN* gene was amplified by PCR with gapN1 and gapN2 primers to add NcoI and KpnI restriction sites at the 5′ and 3′ ends, respectively. The Chloramphenicol resistance cassette flanked by FRT sites (*cat-frt* fragment) was amplified by PCR with cm1 and cm2 primers using the pKD3 plasmid as a template (Datsenko and Wanner 2000). The *cat-frt* fragment contained KpnI and XmaI restriction sites at the 5′ and 3′ ends respectively. The 3′ end of the *gapN* gene and 5′ end of the *cat-frt* fragment was fused through the KpnI restriction site and this construction was named *gapN-cat-frt* cassette. The *gapN-cat-frt* cassette was inserted into the pTrc99A vector (Amann et al. 1988), which was digested with NcoI and XmaI, to generate pTgapN/cat-frt plasmid. The *gapN-cat-frt* cassette was integrated into the *gapA* locus in *E. coli* MG1655 chromosome to allow transcriptional control of *gapN* by the *gapA* promoter region. The *gapN-cat-frt* cassette was amplified from the pTgapN/cat-frt plasmid, using D1 and D2 primers with 50 nucleotides of homology to the *gapA* promoter

sequence and the beginning and end of the *gapN-cat-frt* cassette. *E. coli* MG1655 was transformed with the pKD46 plasmid (Datsenko and Wanner 2000), which promotes homologous recombination at the designed sites of the *gapN-cat-frt* cassette. Recombinant strains were selected on Luria–Bertani (LB) solid medium supplemented with 10 μg mL^{-1} of chloramphenicol. The MG1655*ΔgapA::gapN* mutant selected strain was verified by DNA sequencing with primers S1 (TAACGAATGGATTCTTCACTTACCGGTTCG) and S2 (TATGCAGGGCAGAGGTGGTTTCAAATTCGC), which hybridize at ~ 580 nucleotides upstream and downstream positions, respectively, of *gapA* gene. The chloramphenicol marker was removed in the MG*ΔgapA::gapN* strain, using the procedure reported by Datsenko and Wanner through pCP20 plasmid (Cherepanov and Wackernagel 1995).

Plasmid pACYC184 (Chang and Cohen 1978) was used to overexpress the *gapN* gene. First, this gene was amplified by PCR with oligonucleotides gapN1 and gapN2 that introduce NcoI and KpnI flanking sites to facilitate cloning into plasmid pTrc99A. The resulting plasmid pGapN was used as a PCR template to amplify the *trcgapN* fragment with oligonucleotides Trc1 and gapN2. This fragment was blunt-ligated into pACYC184 previously digested with ScaI to generate plasmid pTrcgapN (Table 1). The construction was verified by digestion with EcoRI and visualized by agarose gel electrophoresis.

Medium and growth conditions

The routine cultivation and genetic manipulation of *E. coli* MG1655 and its mutant were performed in Luria–Bertani medium (10 g L^{-1} tryptone, 5 g L^{-1} yeast extract, and 10 g L^{-1} NaCl, pH 7.2) supplemented with the appropriate antibiotics, when necessary. *S. mutans* strain was cultivated in blood agar (Merk KGaA, Darmstadt Germany) at 37 °C. Cells were harvested in a saline solution (0.9 %) in order to isolate the chromosomal DNA. For characterization of the MG*ΔgapA::gapN* harbouring pTrcgapN plasmid, *E. coli* cultivations were performed in 500 mL shake flasks containing 100 mL of M9 medium, (per liter): 6 g Na_2HPO_4; 3 g KH_2PO_4; 0.5 g NaCl; 1 g NH_4Cl; 2 mM $MgSO_4$; 0.1 mM $CaCl_2$; 0.01 g Vit B1, and 8 g glucose at 37 °C with an agitation of 300 rpm.

To characterize the strains, *E. coli* MG1655Δ*gapA::gapN*/pTrcgapN was compared with *E. coli* MG1655 wild-type strain and MG*ΔgapA::gapN* carrying an empty pACYC184 plasmid. Cultures were performed in pH-controlled fermenters. Seed cells were prepared in a 2.8 L Fermbach flask containing 500 mL of M9 medium with 5 g L^{-1} glucose. The cells from 350 mL of culture were harvested by centrifugation at an OD_{600} of 1 and resuspended with 10 mL of fresh M9 medium; these cells were used as inoculum for the bioreactor. Fermentations were conducted in a 1-L bioreactor (Applikon Biotechnology, Netherlands) with a working volume of 0.7 L, 600 rpm, pH controlled at 7 with NaOH (2N), and an air flow rate of 0.84 L min^{-1}. The samples were collected in the mid-log phase at an OD_{600} of 3 to determine: cofactors, GAPDH enzymatic activity, and RNA extraction for transcriptional analysis. All experiments and analysis were performed in triplicates, figures and tables show averages and standard deviations.

Metabolite analysis and kinetic and stoichiometric parameters

The samples were centrifuged (4 °C), and the cell-free culture broth was frozen for subsequent analysis. The concentration of glucose and acetic acid in the culture broths was quantified using an HPLC (1200, Agilent, CA, USA) equipped with a refractive index detector and an ion-exchange column (50 °C) (300 × 78 mm^2; Aminex HPX-87H; BioRad, USA) using a mobile phase of 0.005 mol L^{-1} H_2SO_4 and a flow rate of 0.5 mL min^{-1} during elution. Respiration rate (q_{O_2}) and CO_2 production rate (q_{CO_2}) were calculated from a mass balance and the composition of inlet and outlet gases from the fermenter and measured by O_2- and CO_2-gas sensors (BlueSens, gas sensor GmbH, Herten, Germany).

The data in figures and tables is the average of at least three different cultures. Cell growth was measured by monitoring the optical density at 600 nm (OD_{600}) in a spectrophotometer (DU-70, Beckman Instruments, Inc. Fullerton, CA, USA). OD_{600} was converted into dry cellular weight (cell concentration) using a calibration curve (1 OD_{600} = 0.42 g L^{-1} of dry cellular weight). The specific growth rates (μ) were determined by fitting the biomass data versus time to exponential regressions. The cell mass yield on glucose ($Y_{X/GLC}$), yield of acetate on glucose ($Y_{ACE/GLC}$), yield of CO_2 ($Y_{CO2/GLC}$) and O_2 ($Y_{02/GLC}$) on glucose were estimated as the coefficient of the linear

regression of the respective metabolite concentration versus the concentration of glucose consumed during the exponential growth phase, in grams of biomass/$mmol_{GLC}$ or $mmol_{PRODUCT}/mmol_{GLC}$. The specific glucose consumption rate (q_s) was determined as the ratio of μ to $Y_{x/s}$. Respiration rate (q_{O_2}) and CO_2 production rate (q_{CO_2}) were calculated from mass balances and the specific growth rate.

Measurements of the intracellular cofactors concentrations during exponential growth phase

The intracellular cofactors, NAD^+, NAD(H), NAD(P)H and $NAD(P)^+$, were extracted and assayed using the EnzyChrom™ assay kit following the supplier's instructions (BioAssay Systems, Hayward, CA, USA). Briefly, three samples of approximately 12.6 mg of wet cells from cultures were immediately received in methanol (70 % v/v) at −50 °C (Lee et al. 2010), for rapid inactivation of the cellular metabolism. The cell pellet was washed with cold PBS and resuspended with base or acid buffer (BioAssay Systems, Hayward, CA, USA) to extract the reduced or oxidized pyridine nucleotides (Bergmeyer 1985). Relative amounts of NAD^+, NADH, $NADP^+$, and NADPH were quantified by enzymatic methods (Bergmeyer 1985) and using $NADP^+$-glucose-6-phosphate dehydrogenase and NAD^+-lactate dehydrogenase (BioAssay Systems, Hayward, CA, USA).

To measure the [ATP]/[ADP] ratio, three samples of ~5 mg of wet cells were received in 2 mL of phenol (equilibrated with 10 mM Tris–1 mM EDTA to pH 8) at 80 °C, samples were treated as reported by Koebbmann (Koebmann et al. 2002). The ATP concentration was then measured by using a luciferin-luciferase kit (ENLITEN® ATP Assay System Bioluminescence Detection kit; Promega Corporation, USA) following the supplier's instructions. Subsequently, the ADP was converted to ATP adding one enzymatic unit of pyruvate kinase and 1 mM phosphoenolpyruvate, then the total ATP was quantified as described above and the ADP concentration was calculated from the difference of both measurements.

Enzymatic assays

The equivalent to 6.3 mg of cells was collected by centrifugation at 4,000×*g* (10 min at 4 °C) and then washed once with cold buffer A (20 mM Tricine buffer, pH 8.5, containing 3 mM 2-mercapto-ethanol). The cells were suspended in 500 μL of the same buffer and sonicated with 3 pulses of 45 s and pauses of 30 s at 4 °C using a sonicator (Soniprep 150 ultrasonic disintegrator, MSE Ltd, London, U.K.). Cell debris was removed by centrifugation (4,000×*g*, 10 min, 4 °C). The resulting supernatant was used for the enzymatic assays. The GAPDH activity was measured as described in (Iddar et al. 2003). The $NADP^+$-GAPDH reaction was started by adding the cell extract to the assay mixture containing buffer A, 1 mM $NADP^+$, and 1 mM D-glyceraldehyde-3-phosphate (G-3-P) at 25 °C. The NAD^+-GAPDH reaction was measured using the same procedure with 1 mM NAD^+ and 10 mM AsO_4^{3-}. The absorbance variation at 340 nm was followed in a spectrophotometer (DU-70, Beckman Instruments, Inc. Fullerton, CA, USA). One specific unit of activity is defined as 1 μmol of NAD(P)H formed per min per mg of protein (IU/mg_{PROT}). The protein concentration was determined by the Bradford method (Bradford 1976) using the Bio-Rad reagent and BSA as standard (Bio-Rad).

RNA extraction, DNAse treatment of RNA and cDNA synthesis for RT-qPCR analysis

Total RNA was isolated and purified using a previously reported method (Aguilar et al. 2012) with the equivalent to 11.1 mg of cells growing logarithmically in the fermenter at an OD_{600nm} of 3. Samples were then suspended in 300 μl of DNAse and RNase-free water (Ambion Inc, Austin, TX, USA) with RNase inhibitor (Fermentas Life Sciences, USA). RNA was analyzed on a formaldehyde agarose gel for integrity. The RNA concentrations were quantified using a Nanodrop (2000c, Thermo Scientific); the 260/280 and 260/230 ratios were examined for protein and solvent contamination. For all samples the 260/280 nm absorbance values were from 1.9 to 2.0 and in the range of 2.0–2.3 for the 260/230 nm ratio. RNA samples were stored at −70 °C. Three RNA extractions and purifications were carried out from three independent fermentations for each strain. For DNAse treatment, total RNA samples were treated with the TURBO DNA-free kit (Ambion Inc, Austin, TX, USA) at 37 °C for 30 min, following the manufacturer's instructions. The cDNA was synthesized using RevertAid™ H minus First Strand cDNA Synthesis kit following the

manufacturer's conditions (Fermentas LifeSciences, USA). For each reaction approximately 5 μg of RNA and a mixture of 10 pmol μL^{-1} of specific DNA reverse primers (b) were used. This cDNA was used as template for RT-qPCR assays. Nucleotide sequences of these primers have been previously published (Flores et al. 2005; Chávez-Béjar et al. 2008; Sigala et al. 2009; Aguilar et al. 2012).

RT-qPCR

RT-qPCR was performed with the ABI Prism 7000 Sequence Detection System and 7300 Real Time PCR System (Perkin Elmer/Applied Biosystems, USA) using the Maxima^R SYBR Green/ROX qPCR Master Mix (2X) kit (Fermentas LifeSciences, USA). MicroAmp Optical 96-well reaction plates (Applied Biosystems, USA) and Plate Max ultraclear sealing films (Axygen Inc, USA) were used in these experiments. All RT-qPCR quantifications were performed as previously reported (Aguilar et al. 2012) and complied with the MIQE guidelines (Minimum Information for Publication of Quantitative Real-Time PCR Experiments) (Bustin et al. 2009; Taylor et al. 2010). The quantification technique used to analyze the data was the $2^{-\Delta\Delta Cq}$ method described by Livak and Shmittgen (2001). For each analyzed gene the transcription levels of the corresponding MG1655 gene were considered equal to one and used as controls to normalize the data. Therefore, data are reported as relative expression levels compared to the expression level of the same gene in strain MG1655, using *ihfB* as housekeeping gene.

Results and discussion

Metabolic responses to *gapN* expression

In order to study the metabolic effects when the NAD$^+$-GAPDH gene from *E. coli* (*gapA*) is replaced with NADP$^+$-GAPDH gene from *S. mutans* (*gapN*), two derivative strains were generated using *E. coli* strain MG1655. Strain MG1655Δ*gapA*::*gapN* was constructed in one step by inserting the *gapN* gene at the same locus as the native *gapA* gene into the chromosome of strain MG1655. In this strain, the *gapN* gene expression was controlled by the *gapA* promoter region (Charpentier and Branlant 1994; Thouvenot et al. 2004). Also, the plasmid pTrcgapN was constructed to overexpress the *gapN* gene from the *trc* promoter (see "Materials and methods" section) and the mutant strain MG1655Δ*gapA::gapN* was transformed with plasmid pTrcgapN (MG1655Δ*gapA::gapN*/pTrcgapN) to increase the *gapN* expression level.

Fermenter batch cultures with mineral medium were carried out supplemented with 8 g L^{-1} of glucose under aerobic conditions. Kinetic data (Fig. 1a, b) showed that the MG1655*ΔgapA::gapN* strain had a specific growth rate (μ) of 0.11 ± 0.03 h^{-1} and a glucose consumption rate (q_s) of 2.06 ± 0.17 $mmol_{glc}\, g_{DCW}^{-1} h^{-1}$ (Table 2). The μ and q_s of MG1655Δ*gapA*::*gapN*/pTrcgapN were 4 and 2.5 times higher than those parameters in MG1655*ΔgapA::gapN*, respectively. Since *E. coli* mutants of the *gapA* gene are unable to grow with hexoses as carbon source (Hillman and Fraenkel 1975; Irani and Maitra 1977; Baba et al. 2006) these data indicate that *gapN* expression can replace the native *gapA* function. Furthermore, the specific NADP$^+$-GAPDH activity of the strain MG1655*ΔgapA::gapN* was 4.6 times lower relative to strain MG1655Δ*gapA*::*gapN*/pTrcgapN (Table 2) and no NAD$^+$-GAPDH activity was detected (Table 2). The specific NADP$^+$-GAPDH activity levels in the derivative strain reveal that growth rate and glucose uptake differences are attributable to *gapN* expression level. Indeed, it has been demonstrated in *E. coli* that carbon flux through the EMP pathway can be controlled through the glyceraldehyde 3-phosphate node by NAD$^+$-GAPDH activity (Cho et al. 2012) and our results show that NADP$^+$-GAPDH heterologous activity can also exert a similar response.

On the other hand, very low acetic acid was produced by strain MG1655*ΔgapA::gapN* (0.04 ± 0.00 $mol_{ACE}\, mol_{GLC}^{-1}$) (Fig. 1c), which is expected since low glucose flux through the EMP pathway prevents the acetic acid synthesis (Hollywood and Doelle 1976; Andersen and von Meyenburg 1980). Moreover, this characteristic is desirable to improve the production of recombinant protein and increase the carbon availability to produce several metabolites (Dittrich et al. 2005; Kern et al. 2007; Waegeman et al. 2013). In contrast, MG1655Δ*gapA*::*gapN*/pTrcgapN directed ~40 % of substrate to acetic acid production (0.78 ± 0.02 $mol_{ACE}\, mol_{GLC}^{-1}$) (Table 2; Fig. 1c). High acetic acid levels were produced when a NADP$^+$-GAPDH from *C. acetobuyiricum* replaced a NAD$^+$-GAPDH from *E. coli* to produce lycopene

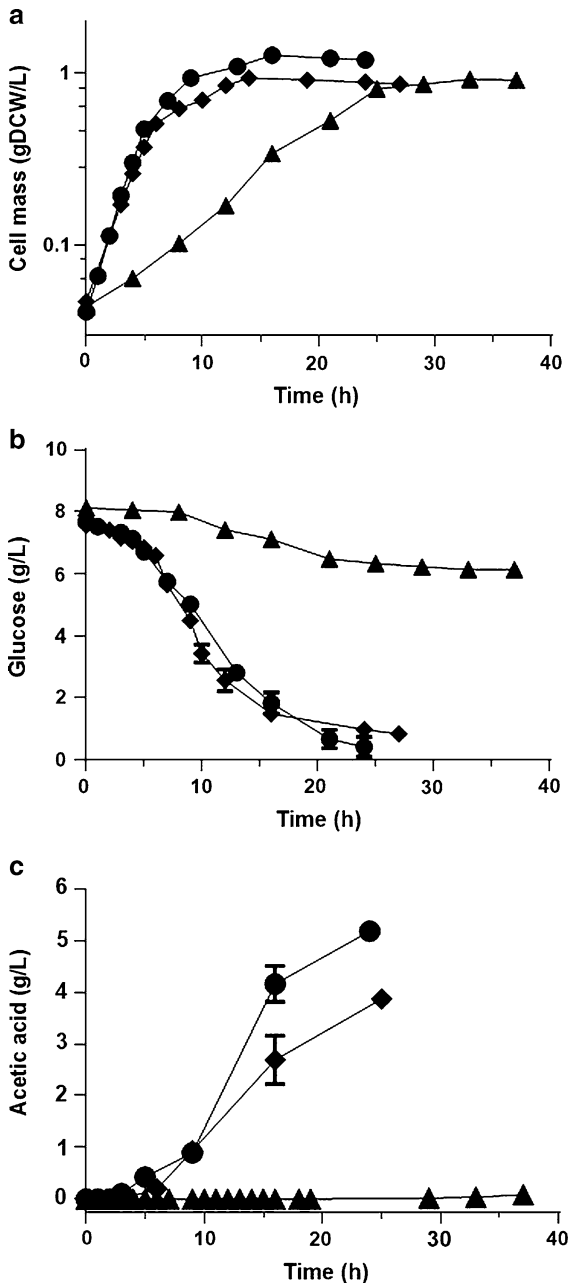

Fig. 1 Kinetic of cell mass formation (**a**), glucose consumption (**b**) and acetic acid production (**c**), strains: MG1655 (*circles*), MG1655*ΔgapA::gapN* (*triangles*) and MG1655*ΔgapA::gapN*/pTrcgapN (*diamonds*)

(Martínez et al. 2008), which could affect the lycopene yield. However, a decrease in acetic acid production is possible by deleting the *ackA-pta* pathway (Phue et al. 2010) or by using a strain with low glycolytic flux (Hollywood and Doelle 1976; Andersen and von Meyenburg 1980) as MG1655Δ*gapA*::*gapN*. These results show that the heterologous $NADP^+$-GAPDH enzyme from *S. mutans* not only replaced the native NAD^+-GAPDH function, but also, as cited above, the carbon flux through the EMP pathway could be controlled by *gapN* expression level, which modulated the glucose uptake and also the acetic acid production rates.

In comparison with the parental strain MG1655, the specific growth and glucose consumption rates in strain MG1655*ΔgapA::gapN* decreased 5 and 3.4 times, respectively (Table 2; Fig. 1a, b). In agreement with that, the specific $NADP^+$-GAPDH activity in strain MG1655*ΔgapA::gapN* was 2.6 times lower than the NAD^+-GAPDH activity in wild-type strain (Table 2). Although the *gapN* gene expression was controlled by the same *gapA* native promoter, the differences in GAPDH activity levels could be attributable to inherent differences in the catalytic properties of each enzyme (D′Alessio and Josse 1971; Crow and Wittenbergerg 1979). In contrast, MG1655Δ*gapA::gapN*/pTrcgapN, has a μ and a q_s 15 and 25 % lower when compared with the wild-type strain (Table 2; Fig. 1a, b). However, the $NADP^+$-GAPDH activity was 1.8 times higher than the NAD^+-GAPDH activity in the parental strain (Table 2). This means that the increase of $NADP^+$-GAPDH heterologous activity can partially restore growth and glucose uptake of the MG1655 strain. In order to elucidate the metabolic effects when NADPH is produced instead of NADH via glyceraldehyde 3-phosphate oxidation, the cofactor levels, transcriptional response and respiration rate were determined in MG1655Δ*gapA::gapN*/pTrcgapN.

Metabolic and transcriptional responses to replacement of NAD^+-GAPDH by $NADP^+$-GAPDH activity

As shown in Fig. 2, the NADH/NAD^+ ratio in the strain MG1655Δ*gapA::gapN*/pTrcgapN decreased 25 % as compared to wild-type strain. In contrast, the NADPH/$NADP^+$ ratio increased 2 times indicating that the alteration in the turnover of NAD(P)H via glyceraldehyde 3-phosphate oxidation affected the redox levels of the strain MG1655Δ*gapA::gapN*/pTrcgapN, which increased 2.8-times the NADPH/NADH ratio (Fig. 2). Concomitantly, the ATP/ADP

Table 2 Growth parameters of the strains MG1655*ΔgapA::gapN*, MG1655*ΔgapA::gapN*/pTrcgapN and MG1655 from batch cultures in glucose-mineral medium

Strain	μ (h^{-1})	q_s ($mmol_{GLC}$ g_{DCW}^{-1} h^{-1})	$Y_{ACE/GLC}$ (mol_{ACE} mol_{GLC}^{-1})	NAD^+-GAPDH activity IU/mg_{PROT}	$NADP^+$-GAPDH activity IU/mg_{PROT}
MG1655*ΔgapA::gapN*	0.11 (0.03)	2.06 (0.17)	0.04 (0.00)	ND	0.201 (0.13)
MG1655*ΔgapA::gapN* /pTrcgapN	0.44 (0.01)	5.24 (0.13)	0.78 (0.02)	ND	0.937 (0.04)
MG1655	0.52 (0.01)	7.04 (0.05)	0.61 (0.07)	0.522 (0.21)	ND

Values in parenthesis indicate the standard deviations

ND Not detected

ratio in the MG1655Δ*gapA::gapN*/pTrcgapN strain decreased 2 times when compared to that of the parental strain (Fig. 2). Moreover, the transcriptional analysis revealed that the expression level of the genes related to the respiratory chain and oxidative phosphorylation such as *nuo* (NADH:ubiquinone oxidoreductase I), *ndh* (ubiquinone oxidoreductase II), *cydA* (cytochrome *bd* oxidase subunit I), *cyoB* (cytochrome *bo* oxidase subunit I) and *atpA* (ATP syntase F_1 complex subunit I) decreased about 50 % in relation to the expression of these genes in the control strain (Fig. 3b). In agreement, several studies have demonstrated that the alteration in the energy levels disturbs the expression of respiration and oxidative phosphorylation genes (Jensen and Michelsen 1992; Noda et al. 2006). Accordingly, the specific respiration rate (q_{O_2}) and yield of consumed oxygen on glucose decreased ($Y_{O2/GLC}$) ~20 and 40 % respectively (Table 3). Since the production of NADH is coupled to the respiratory chain to provide ATP through oxidative phosphorylation (Andersen and von Meyenburg 1980; Koebmann et al. 2002; Vemuri et al. 2006; Holm et al. 2010), these data suggest that the decreased respiration and energy levels were caused by a decrease in the expression of the respiratory and oxidative phosphorylation genes as a response to low NADH production.

Interestingly, the expression of the genes that code for the succinate dehydrogenase A and C (*sdhA* and *sdhC* respectively) and fumarase A (*fumA*) and fumarase B (*fumB*) were also increased more than 60 % when compared with the control strain (Fig. 3a, b). SdhA and SdhB are involved in complex II of the respiratory chain using $FADH_2$ as an electron donor (Brandsch 1989), while FumA and FumB produce NADH across the cytoplasmic membrane (Yagi and Matsuno-yagi 2003). The expression of both systems

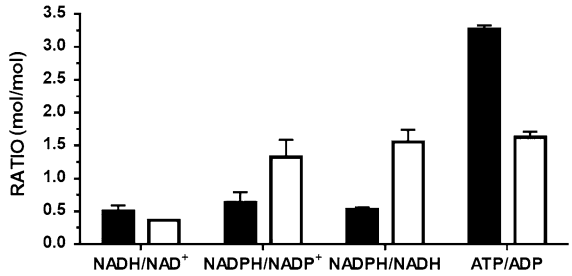

Fig. 2 NADPH/$NADP^+$, NADH/NAD^+, NADPH/NADH and ATP/ADP ratios (mol/mol) of strains MG1655 (*fill*) and MG1655*ΔgapA::gapN*/pTrcgapN (*empty*)

depends on the intracellular NADH state, determined by the type of carbon source or by oxygen presence (Kalman and Gunsalus 1988; Bogaerts et al. 1995). Because the NADH levels were altered in MG1655Δ*gapA::gapN*/pTrcgapN, it is possible that the expression of these oxidoreductases acts as a response to the low NADH levels.

On the other hand, transcriptional analysis indicated that the expression of genes from the EMP in MG1655Δ*gapA::gapN*/pTrcgapN did not significantly change (>0.5 relative to parental strain) (Fig. 3a). This was expected since the expression of glycolytic genes depends on global transcriptional regulators such as Crp, which responds when the carbon uptake is limited (Takahashi et al. 1998) and as was shown, is not the case of MG1655Δ*gapA::gapN*/pTrcgapN.

The expression of the *udhA* gene, encoding transhydrogenase UdhA, increased 2.4 times in the MG1655Δ*gapA::gapN*/pTrcgapN strain (Fig. 3c) presumably to generate NADH from an excess of NADPH (Canonaco et al. 2001; Sauer et al. 2004; Holm et al. 2010; Charusanti et al. 2010). Likewise,

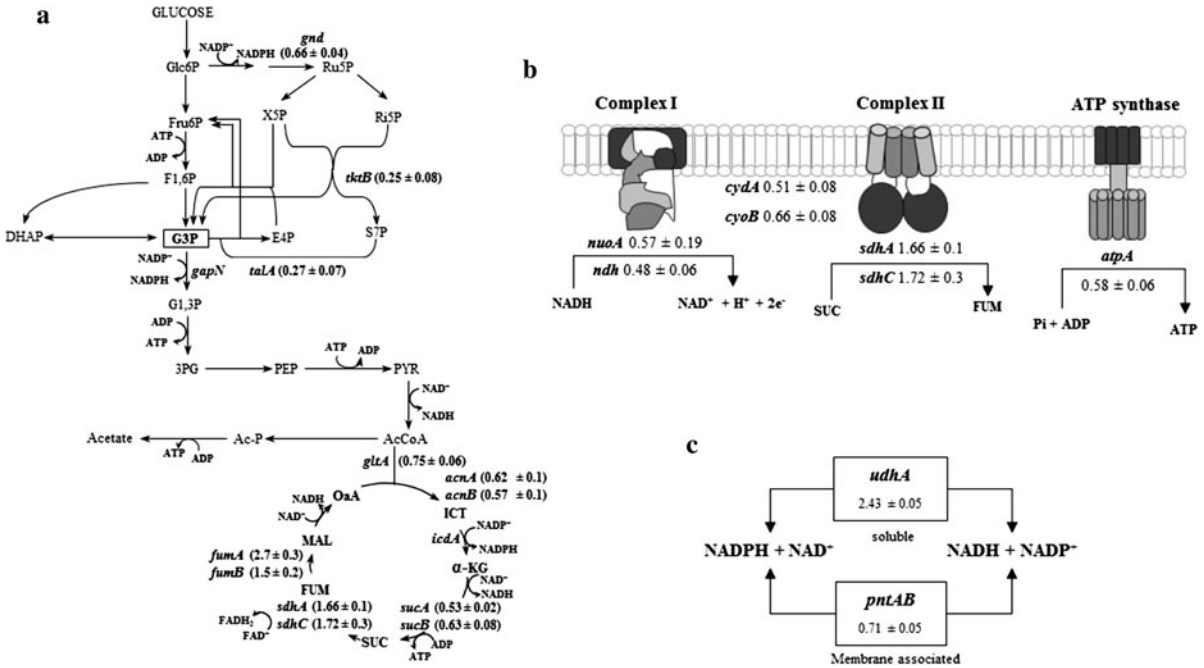

Fig. 3 Transcript levels of genes involved in: carbon central metabolism (**a**), respiratory chain-oxidative phosphorylation (**b**) and transhydrogenase system (**c**) in MG*ΔgapA::gapN*/pTrcgapN strain. The values are expressed relative to the wild-type strain MG1655. According to the significance criterion, only those relative gene transcription values $\geq$1.5 (up-regulation) or $\leq$0.5 (down-regulation), when compared to the MG1655 reference strain, are shown. Metabolite abbreviations: Embden-Meyerhof-Parnas Pathway: *Glc6P* glucose-6-phosphate, *Fru6P* fructose-6-phosphate, *F1,6P,* fructose-1,6-biphosphate, *DHAP* dihydroxyacetone phosphate, *G3P* glyceraldehyde 3-phosphate, *G1,3P* 1,3-biphosphoglycerate, *3PG* 3-phosphoglycerate, *PEP* phosphoenolpyruvate, *PYR* pyruvate. Pentoses Phosphate Pathway: *Ru5P* ribulose-5-phosphate, *Ri5P* ribose-5-phosphate, *X5P* xylulose-5-phosphate, *S7P* sedoheptulose-7-phosphate, *E4P* erythrose-4-phosphate. Tricarboxylic Acid Cycle: *AcCoA* acetyl coenzyme A, *ICT* isocitrate, *α-KG* α-ketoglutarate, *SUC* succinate, *FUM* fumarate, *MAL* malate, *OaA* oxaloacetate. Acetic Acid Pathway: *Ac–P* acetyl phosphate

Table 3 Kinetic parameters of strains MG1655 and MG1655*ΔgapA::gapN*/pTrcgapN from batch cultures in glucose mineral medium

Strain	q_{O_2} ($mmol_{O2}$ g_{DCW}^{-1} h^{-1})	q_{CO_2} ($mmol_{CO2}$ g_{DCW}^{-1} h^{-1})	q_{ACE} ($mmol_{ACE}$ g_{DCW}^{-1} h^{-1})	$Y_{CO2/GLC}$ (mol mol^{-1})	$Y_{O2/GLC}$ (mol mol^{-1})	$Y_{ACE/GLC}$ (mol_{ACE} mol_{GLC}^{-1})
MG1655	16.98	16.84	4.97	0.88	0.92	0.61
	(0.35)	(0.25)	(0.32)	(0.02)	(0.03)	(0.07)
MG1655	14.01	13.89	4.85	0.54	0.55	0.78
ΔgapA::gapN/pTrcgapN	(0.26)	(0.16)	(0.45)	(0.03)	(0.03)	(0.02)

Values in parenthesis indicate the standard deviations

the expression of key genes from the oxidative branch of PPP pathway such as *gnd* (6-phosphogluconate dehydrogenase), *tktB* (transketolase II) and transaldolase A (*talA*) decreased around 34 and 75 % when compared to the parental strain (Fig. 3a), suggesting a low activity of the oxidative branch of PPP. Because PPP is one of the most important routes to produce NADPH (Csonka and Fraenkel 1977; Fuhrer and Sauer 2009), these data concur with the previous observation that high NADPH levels decrease carbon flux through PPP (Kabir and Shimizu 2003; Martínez et al. 2008).

The expression of genes involved in directing acetyl-CoA through TCA cycle such as *gltA* (citrate synthase), *acnA* (aconitate hydratase 1), *acnB* (bifunctional aconitate hydratase 2 and 2-methylisocitrate dehydratase), *sucA* (2-oxoglutarate decarboxylase) and *sucB* (dihydrolipoyltranssuccinylase) were ~50 % downexpressed in the MG1655Δ*gapA::gapN*/pTrcgapN strain (Fig. 3a) suggesting that the TCA cycle was less active than in the parental strain. Furthermore, the moles of CO_2 produced per mole of glucose consumed decreased 39 % in MG1655Δ*gapA::gapN*/pTrcgapN strain (Table 3). Concomitantly, the acetic acid yield on glucose ($Y_{Ace/Glc}$) was 22 % higher in MG1655Δ*gapA::gapN*/pTrcgapN when compared to the parental strain. Such data indicate that in strain MG1655Δ*gapA::gapN*/pTrcgapN more acetyl-CoA was directed to produce acetic acid instead of entering the TCA cycle, this could be a response to increase ATP levels via AckA-Pta and reduce NADPH production by isocitrate dehydrogenase activity (IcdA). A similar observation was reported by Martinez et al., showing that an *E. coli* Δ*gapA*::*gapC* mutant also exhibited low flux through the acetyl-CoA node (Martínez et al. 2008).

Conclusions

The $NADP^+$-GAPDH from *S. mutans* replaced the NAD^+-GAPDH native function in *E. coli*. The growth, glucose uptake and acetic acid production rates were controlled by the $NADP^+$-GAPDH heterologous activity level. Although the overexpression of the $NADP^+$-GAPDH gene can restore the growth in the NAD^+-GAPDH mutant to similar levels as those shown by the wild type strain, the replacement increased the NADPH levels with a concomitant decrease in the NADH levels. The metabolic and transcriptional analysis indicated that the redox perturbation restricted NADPH production through other native pathways and limited respiratory capabilities, decreasing the energy levels.

Acknowledgments We gratefully acknowledge Georgina Hernández-Chávez, Luz María Martínez, Mercedes Enzaldo, Ramón de Anda and Adelfo Escalante for technical assistance. We thank Martha Giles (Facultad de Química—Universidad Nacional Autónoma de México) for providing the *Streptococcus mutans* strain. This work was supported by the Mexican Council of Science and Technology (CONACyT). SC-L held a scholarship from CONACyT.

References

Aguilar C, Escalante A, Flores N et al (2012) Genetic changes during a laboratory adaptive evolution process that allowed fast growth in glucose to an *Escherichia coli* strain lacking the major glucose transport system. BMC Genom 13:385

Amann E, Ochs B, Abel K (1988) Tightly regulated tac promoter vectors useful for the expression of unfused and fused proteins in *Escherichia coli*. Gene 69:301–315

Andersen KB, von Meyenburg K (1980) Are growth rates of *Escherichia coli* in batch cultures limited by respiration? J Bacteriol 144:114–123

Baba T, Ara T, Hasegawa M et al (2006) Construction of *Escherichia coli* K-12 in-frame, single-gene knockout mutants: the Keio collection. Mol Syst Biol 2:2006.0008

Bergmeyer H (1985) Methods of enzymatic analysis, 3rd edn. VCH Verlagsgesellschaft mbH, Weinheim

Bogaerts J, Zoske S, Weidner U, Linden G (1995) Transcriptional regulation of the proton translocating NADH dehydrogenase (*nuoA-N*) of *Escherichia coli* by electron acceptors, electron donors and gene regulators. Mol Microbiol 16:521–534

Boyd DA, Cvitkovitch DG, Hamilton IANR (1995) Sequence, expression, and function of the gene for the phosphate dehydrogenase of *Streptococcus mutans*. J Bacteriol 177: 2622–2627

Bradford M (1976) A rapid and sensitive method for the quantitation of microgram quantities of protein utilizing the principle of protein-dye binding. Anal Biochem 72: 248–254

Brandsch R (1989) Covalent cofactor binding to flavoenzymes requires specific effectors. Eur J Biochem 182:125–128

Brown AT, Wittenberger CL (1971) Mechanism for regulating the distribution of glucose carbon between the Embden-Meyerhof and hexose-monophosphate pathways in *Streptococcus faecalis*. J Bacteriol 106:456–467

Bustin SA, Benes V, Garson JA et al (2009) The MIQE guidelines: minimum information for publication of quantitative real-time PCR experiments. Clin Chem 55:611–622

Canonaco F, Hess TA, Heri S et al (2001) Metabolic flux response to phosphoglucose isomerase knock-out in *Escherichia coli* and impact of overexpression of the soluble transhydrogenase UdhA. FEMS Microbiol Lett 204:247–252

Chang ACY, Cohen SN (1978) Construction and characterization of amplifiable multicopy DNA cloning vehicles derived from the P15A cryptic miniplasmid. J Bacteriol 134:1141–1156

Charpentier B, Branlant C (1994) The *Escherichia coli gapA* gene is transcribed by the vegetative RNA polymerase holoenzyme Eσ70 and by the heat shock RNA polymerase Eσ32. J Bacteriol 176:830–839

Charusanti P, Conrad TM, Knight EM et al (2010) Genetic basis of growth adaptation of *Escherichia coli* after deletion of *pgi*, a major metabolic gene. PLoS Genet 6(11):e1001186

Chávez-Béjar M, Lara AR, López H et al (2008) Metabolic engineering of *Escherichia coli* for L -tyrosine production by expression of genes coding for the chorismate mutase domain of the native chorismate mutase-prephenate dehydratase and a cyclohexadienyl dehydrogenase from

Zymomonas mobilis. Appl Environ Microbiol 74:3284–3290

Cherepanov PP, Wackernagel W (1995) Gene disruption in *Escherichia coli*: Tc^R and Km^R cassettes with the option of Flp-catalyzed excision of the antibiotic-resistance determinant. Gene 158:9–14

Cho H-S, Seo SW, Kim YM et al (2012) Engineering glyceraldehyde-3-phosphate dehydrogenase for switching control of glycolysis in *Escherichia coli*. Biotechnol Bioeng 109:2612–2619

Crow L, Wittenbergerg CL (1979) Separation and properties of NAD+- and NADP+-dependent glyceraldehyde-3-phosphate dehydrogenases from *Streptococcus mutans*. J Biol Chem 254:1134–1142

Csonka LN, Fraenkel DG (1977) Pathways of NADPH formation in *Escherichia coli*. J Biol Chem 252:3382–3391

D′Alessio G, Josse J (1971) Glyceraldehyde phosphate dehydrogenase of *Escherichia coli*. J Biol Chem 246:4326–4333

Datsenko K, Wanner BL (2000) One-step inactivation of chromosomal genes in *Escherichia coli* K-12 using PCR products. Proc Natl Acad Sci USA 97:6640–6645

Dittrich CR, Vadali RV, Bennett GN, San K (2005) Redistribution of metabolic fluxes in the central aerobic metabolic pathway of *E. coli* mutant strains with deletion of the *ackA-pta* and *poxB* pathways for the synthesis of isoamyl acetate. Biotechnol Prog 21:627–631

Fillinger S, Boschi-Muller S, Azza S et al (2000) Two glyceraldehyde-3-phosphate dehydrogenases with opposite physiological roles in a nonphotosynthetic bacterium. J Biol Chem 275:14031–14037

Flores N, Flores S, Escalante A et al (2005) Adaptation for fast growth on glucose by differential expression of central carbon metabolism and gal regulon genes in an *Escherichia coli* strain lacking the phosphoenolpyruvate:carbohydrate phosphotransferase system. Metab Eng 7:70–87

Foster JW, Park YK, Penfound T et al (1990) Regulation of NAD metabolism in *Salmonella typhimurium*: molecular sequence analysis of the bifunctional *nadR* regulator and the *nadA-pnuC* operon. J Bacteriol 172:4187–4196

Fuhrer T, Sauer U (2009) Different biochemical mechanisms ensure network-wide balancing of reducing equivalents in microbial metabolism. J Bacteriol 191:2112–2121

Habenicht A (1997) The non-phosphorylating glyceraldehyde-3-phosphate dehydrogenase: biochemistry, structure, occurrence and evolution. Biol Chem 378:1413–1419

Hillman JD, Fraenkel DG (1975) Glyceraldehyde 3-phosphate dehydrogenase mutants of *Escherichia coli*. J Bacteriol 122:1175–1179

Hollywood N, Doelle H (1976) Effect of specific growth rate and glucose concentration on growth and glucose metabolism of *Escherichia coli* K-12. Microbios 17:23–33

Holm AK, Blank LM, Oldiges M et al (2010) Metabolic and transcriptional response to cofactor perturbations in *Escherichia coli*. J Biol Chem 285:17498–17506

Iddar A, Valverde F, Serrano A, Soukri A (2002) Expression, purification, and characterization of recombinant non-phosphorylating NAP-dependent glycerladehyde-3-phosphate dehydrogenase from *Clostridium acetobutylicum*. Protein Expr Purif 25:519–526

Iddar A, Valverde F, Serrano A, Soukri A (2003) Purification of recombinant non-phosphorylating NADP-dependent glyceraldehyde-3-phosphate dehydrogenase from *Streptococcus pyogenes* expressed in *E. coli*. Mol Cell Biochem 247:195–203

Iddar A, Valverde F, Assobhei O et al (2005) Widespread occurrence of non-phosphorylating dehydrogenase among Gram-positive bacteria. Int Microbiol 8:251–258

Irani MH, Maitra PK (1977) Properties of *Escherichia coli* mutants deficient in enzymes of glycolysis. J Bacteriol 132:398–410

Jensen PR, Michelsen OLE (1992) Carbon and energy metabolism of *atp* mutants of *Escherichia coli*. J Bacteriol 174:7635–7641

Kabir MM, Shimizu K (2003) Fermentation characteristics and protein expression patterns in a recombinant *Escherichia coli* mutant lacking phosphoglucose isomerase for poly(3-hydroxybutyrate) production. Appl Environ Microbiol 62:244–255

Kalman LV, Gunsalus RP (1988) The *frdR* Gene of *Escherichia coli* globally regulates several operons involved in anaerobic growth in response to nitrate. J Bacteriol 170:623–629

Kern A, Tilley E, Hunter IS et al (2007) Engineering primary metabolic pathways of industrial micro-organisms. J Biotechnol 129:6–29

Kim S, Moon D-B, Lee C-H et al (2009) Comparison of the effects of NADH- and NADPH-perturbation stresses on the growth of *Escherichia coli*. Curr Microbiol 58:159–163

Kim S, Lee CH, Nam SW, Kim P (2011) Alteration of reducing powers in an isogenic phosphoglucose isomerase (pgi)-disrupted *Escherichia coli* expressing NAD(P)-dependent malic enzymes and NADP-dependent glyceraldehyde 3-phosphate dehydrogenase. Lett Appl Microbiol 52:433–440

Kocharin K, Siewers V, Nielsen J (2013) Improved polyhydroxybutyrate production by *Saccharomyces cerevisiae* through the use of the phosphoketolase pathway. Biotechnol Bioeng 110:2216–2224

Koebmann BJ, Westerhoff HV, Snoep JL et al (2002) The glycolytic flux in *Escherichia coli* is controlled by the demand for ATP. J Bacteriol 184:3909–3916

Lee HC, Kim JS, Jang W, Kim SY (2010) High NADPH/NADP+ ratio improves thymidine production by a metabolically engineered *Escherichia coli* strain. J Biotechnol 149:24–32

Livak KJ, Schmittgen TD (2001) Analysis of relative gene expression data using real-time quantitative PCR and the 2(−Delta Delta C(T)) method. Methods 25:402–408

Marchal S, Branlant G (2002) Characterization of the amino acids involved in substrate specificity of nonphosphorylating glyceraldehyde-3-phosphate dehydrogenase from *Streptococcus mutans*. J Biol Chem 277:39235–39242

Martínez I, Zhu J, Lin H et al (2008) Replacing *Escherichia coli* NAD-dependent glyceraldehyde 3-phosphate dehydrogenase (GAPDH) with a NADP-dependent enzyme from *Clostridium acetobutylicum* facilitates NADPH dependent pathways. Metab Eng 10:352–359

Moat AG, Foster JW, Spector MP (2002) Fermentation pathways. Microbial Physiology p 412–433

Noda S, Takezawa Y, Mizutani T et al (2006) Alterations of cellular physiology in *Escherichia coli* in response to

oxidative phosphorylation impaired by defective F1-ATPase. J Bacteriol 188:6869–6876

Phue J-N, Lee SJ, Kaufman JB et al (2010) Acetate accumulation through alternative metabolic pathways in *ackA*$^-$ *pta*$^-$ *poxB*$^-$ triple mutant in *E. coli* B (BL21). Biotechnol Lett 32:1897–1903

Sambrook J, Rusell D (2001) Molecular cloning a laboratory manual, 3rd edn. Cold Spring Harbor Laboratory Press, Cold Spring Harbor

Sauer U, Canonaco F, Heri S et al (2004) The soluble and membrane-bound transhydrogenases UdhA and PntAB have divergent functions in NADPH metabolism of *Escherichia coli*. J Biol Chem 279:6613–6619

Sigala JC, Flores S, Flores N et al (2009) Acetate metabolism in *Escherichia coli* strains lacking phosphoenolpyruvate: carbohydrate phosphotransferase system; evidence of carbon recycling strategies and futile cycles. J Mol Microbiol Biotechnol 16:224–235

Takahashi H, Inada T, Postma P, Aiba H (1998) CRP down-regulates adenylate cyclase activity by reducing the level of phosphorylated IIA(Glc), the glucose-specific phosphotransferase protein, in *Escherichia coli*. Mol Gen Genet 259:317–326

Takeno S, Murata R, Kobayashi R et al (2010) Engineering of *Corynebacterium glutamicum* with an NADPH-generating glycolytic pathway for L-lysine production. Appl Environ Microbiol 76:7154–7160

Taylor S, Wakem M, Dijkman G et al (2010) A practical approach to RT-qPCR-publishing data that conform to the MIQE guidelines. Methods 50:S1–S5

Thouvenot B, Charpentier B, Branlant C (2004) The strong efficiency of the *Escherichia coli gapA* P1 promoter depends on a complex combination of functional determinants. Biochem J 382:371–382

Valverde F, Losada M, Serrano A (1999) Engineering a central metabolic pathway: glycolysis with no net phosphorylation in an *Escherichia coli gap* mutant complemented with a plant *gapN* gene. FEBS Lett 449:153–158

Vemuri GN, Altman E, Sangurdekar DP et al (2006) Overflow metabolism in *Escherichia coli* during steady-state growth: transcriptional regulation and effect of the redox ratio. Appl Environ Microbiol 72:3653–3661

Waegeman H, De Lausnay S, Beauprez J et al (2013) Increasing recombinant protein production in *Escherichia coli* K12 through metabolic engineering. N Biotechnol 30:255–261

Yagi T, Matsuno-yagi A (2003) The proton-translocating NADH-quinone oxidoreductase in the respiratory chain: the secret unlocked. Biochemistry 42:2266–2274